

**Interpretation of
Cluster WBD
frequency conversion
mode data**

J. S. Pickett et al.

Interpretation of Cluster WBD frequency conversion mode data

J. S. Pickett, I. W. Christopher, and D. L. Kirchner

The University of Iowa, Iowa City, Iowa, 52242, USA

Received: 31 May 2013 – Accepted: 6 August 2013 – Published: 29 August 2013

Correspondence to: J. S. Pickett (pickett@uiowa.edu)

Published by Copernicus Publications on behalf of the European Geosciences Union.

[Title Page](#)

[Abstract](#)

[Introduction](#)

[Conclusions](#)

[References](#)

[Tables](#)

[Figures](#)



[Back](#)

[Close](#)

[Full Screen / Esc](#)

[Printer-friendly Version](#)

[Interactive Discussion](#)

Abstract

The Cluster Wide-Band Data (WBD) plasma wave receiver mounted on each of the four Cluster spacecraft obtains high time resolution waveform data in the frequency range of ~ 70 Hz to 577 kHz. In order to make measurements above 77 kHz, it uses frequency conversion to sample the higher frequency waves at one of three different conversion frequencies (~ 125 , 250 and 500 kHz, where these frequencies are the base frequency of the frequency range being sampled) in one of three different filter bandwidths (9.5, 19 and 77 kHz). Within the WBD instrument a down conversion technique, built around quadrature mixing, is used to convert these data to baseband (0 kHz) in order to reduce the sample rate for telemetry to the ground. We describe this down conversion technique and illustrate it through data obtained in space. Because these down converted data sometimes contain pulses, which can be indicative of nonlinear physical structures (e.g., electron phase space holes and electron density enhancements and depletions), it is necessary to understand what effects mixing and down conversion have on them. We present simulations using constructed signals containing pulses, nonlinear wave packets, sinusoids and noise. We show that the pulses and impulsive wave packets, if of sufficient amplitude and of appropriate width, survive the down conversion process, sometimes with the same pulse shape but usually with reduced amplitude, and have time scales consistent with the filter bandwidth at the base frequency. Although we cannot infer the actual time scale of the pulses and impulsive wave packets as originally recorded by the WBD instrument before mixing and down conversion, their presence indicates nonlinear processes occurring at or somewhat near the location of the measurement. Sinusoidal waves are represented in the down conversion time scale as sinusoids of nearly the same amplitude and at frequencies adjusted down by the conversion frequency. The original input waveforms, regardless of their shape, whether pulses or sinusoids, can never be recovered from the down converted waveforms.

Interpretation of Cluster WBD frequency conversion mode data

J. S. Pickett et al.

[Title Page](#)

[Abstract](#)

[Introduction](#)

[Conclusions](#)

[References](#)

[Tables](#)

[Figures](#)



[Back](#)

[Close](#)

[Full Screen / Esc](#)

[Printer-friendly Version](#)

[Interactive Discussion](#)



1 Introduction

Each of the four spacecraft that comprise the ESA/NASA Cluster mission contains an identical Wide-Band Data (WBD) plasma wave receiver, providing high time resolution waveform data from ~ 70 Hz up to 577 kHz (Gurnett et al., 1997). The waveform data obtained from these instruments are telemetered directly to ground stations allowing for sample rates of ~ 27 – 220 kHz depending on the detection frequency bandwidth, f_{BW} (9.5, 19, or 77 kHz) and resolution (1, 4 or 8 bit) modes which have been chosen. In order to obtain waveform data at frequencies higher than 77 kHz, the WBD instrument design allows the input frequency range to be shifted by a frequency converter to one of four frequency ranges. The conversion frequency, f_0 , determines the lower edge of the frequency range selected. The available values of f_0 are 0 (or baseband), 125, 250 or 500 kHz (approximate values, the exact values being provided in the Cluster WBD User Guide archived at the Cluster Final Archive), so the digitized frequency range is then f_0 to $f_0 + f_{\text{BW}}$. Both the sampling frequency and f_0 are obtained by division from a 14 MHz reference oscillator contained within the WBD instrument. The oscillator is phase-locked to the spacecraft 220.753 kHz high frequency clock to maintain stability and match the instrument data rate to the spacecraft. The spacecraft Ultra-Stable Oscillator, operating at a frequency of 2^{22} Hz, is divided by 19 to derive the high frequency clock, so WBD data are sampled with phase coherence to spacecraft timing.

If baseband ($f_0 = 0$) is selected, the down conversion stage is bypassed and the WBD signal in the frequency range 0 to f_{BW} is routed directly to the digitizer with no frequency conversion. When $f_0 \neq 0$, frequency translation is used to convert the input signal $[f_0 \pm f_{\text{BW}}]$ to baseband (see Fig. 1). Note that hereinafter brackets will be used to indicate a range of frequencies, either a double sideband range $[f_0 \pm f_{\text{BW}}]$ ($f_0 - f_{\text{BW}}$ to $f_0 + f_{\text{BW}}$), or a single sideband range such as $[f_0 - f_{\text{BW}}](f_0 - f_{\text{BW}}$ to $f_0)$. Since only the upper sideband $[f_0 + f_{\text{BW}}]$ is the desired output, a quadrature mixer is used for single sideband detection. The quadrature mixer multiplies the input signal by f_0 in two channels, one using f_0 (the “I” or “In-phase” channel) and the other using f_0 phase shifted

Interpretation of Cluster WBD frequency conversion mode data

J. S. Pickett et al.

[Title Page](#)

[Abstract](#)

[Introduction](#)

[Conclusions](#)

[References](#)

[Tables](#)

[Figures](#)

[⏪](#)

[⏩](#)

[◀](#)

[▶](#)

[Back](#)

[Close](#)

[Full Screen / Esc](#)

[Printer-friendly Version](#)

[Interactive Discussion](#)

Interpretation of Cluster WBD frequency conversion mode data

J. S. Pickett et al.

[Title Page](#)

[Abstract](#)

[Introduction](#)

[Conclusions](#)

[References](#)

[Tables](#)

[Figures](#)

[⏪](#)

[⏩](#)

[◀](#)

[▶](#)

[Back](#)

[Close](#)

[Full Screen / Esc](#)

[Printer-friendly Version](#)

[Interactive Discussion](#)



by 90 degrees (the “Q” or “Quadrature phase” channel). The two resulting baseband signals each contain the frequency range $[f_0 \pm f_{BW}]$. To cancel the unwanted sideband $[f_0 - f_{BW}]$, both channels are processed through two high precision passive phase shift networks. The phase shift lattice is a three port device, with one input and two outputs, which differ from each other by 90° . In the I channel, the 0° output is selected, while in the Q channel, the 90° output is used. The 90° phase shift added to the Q channel output shifts the positive sideband $[f_0 + f_{BW}]$ into phase coherence with the $[f_0 + f_{BW}]$ signal in the I channel, while the same shift moves the lower sideband $[f_0 - f_{BW}]$ into interference with the $[f_0 - f_{BW}]$ signal in the I channel. Summing the two selected outputs then cancels the unwanted lower sideband (Norgaard, 1956). The lower sideband could be selected by differencing the two outputs. The high precision network allows sideband cancellation exceeding the 48 dB capability of the 8 bit A/D converter. This technique allows a significant reduction in cost and mass over the alternative procedure of procuring filters with sufficient selectivity to eliminate the unwanted lower sideband.

The down conversion process preserves the frequency information in the signal, but it does not necessarily preserve the shape of the waveform, particularly when the frequency content of the signal is significantly filtered during bandpass filtering. Since the process is inherently Fourier in nature, pulses and other non-sinusoidal wave features may well be distorted. In order to better understand what happens to pulses undergoing this process and thus how to interpret the results, we have simulated the mixing and down conversion process that takes place within the WBD instrument by creating an artificial signal similar to what is observed by WBD in space.

The primary reason for requiring frequency conversion is to enable detection of high frequency radio waves where direct sampling would exceed the allowable data rate to the spacecraft. The down conversion process that takes place onboard within the WBD instrument allows the selected detection band $[f_0$ to $f_{BW}]$ to be shifted down in frequency to baseband and in so doing reduce the needed sample rate to one which fits the spacecraft telemetry system allocation. For example, in the case of the WBD $f_0 = 125$ kHz conversion mode using the 77 kHz filter bandwidth, the unconverted in-

this region were the sinusoidal signatures of the AKR, but also very short time duration pulses which have not previously been discussed in the literature due to the limitations of most instrumentation to detect them on very short time scales.

Figure 2b is a frequency-time spectrogram covering a period of 2 s during which time Cluster spacecraft 1 transited the auroral upward current region at $2.2 R_E$ (~ 7600 km altitude). These data were obtained by the WBD receiver on 24 January 2010 in the form of waveforms in the 125 kHz conversion mode with a 77 kHz filter bandwidth, with 2180 samples being obtained over an approximate 10 ms period every 80 ms. As described above, the data were down converted to baseband within the instrument, before being transmitted to the ground, and then were analysed by first calibrating them to electric field units of mV/m. Then an FFT was applied to each set of 1090 samples, thereby obtaining the frequency components in the baseband frequency domain (0–77 kHz) and with amplitudes in $\text{mV}^2 \text{m}^{-2} \text{Hz}^{-1}$. In order to put these data back into the frequency range in which they were obtained in space, as opposed to that of baseband as they were telemetered to the ground, we now add the conversion factor, 125 kHz, to the frequency label of each Fourier component, in essence up converting to the measured frequency domain. The amplitudes at each frequency, represented by color in Fig. 2b, are in units of electric field spectral density. Prominent in Fig. 2b are AKR emissions around 192 kHz. Also prominent in this figure is a broad band that covers all frequencies at around 03:46:25.9 UT.

Plotted in Fig. 2a is a $10 \mu\text{s}$ sample of the waveforms obtained during the time of the data shown in Fig. 2b. These data show a pulse at 03:46:25.962054 UT, which is the cause of the broad band observed in Fig. 2b since the Fourier transform of a pulse will contain a wide range of frequencies, depending on pulse shape and width. Also apparent in Fig. 2b are the sinusoidal waves associated with the AKR around 192 kHz. A crude analysis of Fig. 2a shows that from 0.0045 to 0.0048 s, or a period of 0.0003 s, there are 20 wave periods. Dividing the number of wave periods by the time duration over which they are observed yields a frequency of 66.7 kHz. This makes it apparent that the time scale shown on the horizontal axis in Fig. 2a is that of baseband since we

GID

3, 547–565, 2013

Interpretation of Cluster WBD frequency conversion mode data

J. S. Pickett et al.

[Title Page](#)

[Abstract](#)

[Introduction](#)

[Conclusions](#)

[References](#)

[Tables](#)

[Figures](#)

[⏪](#)

[⏩](#)

[◀](#)

[▶](#)

[Back](#)

[Close](#)

[Full Screen / Esc](#)

[Printer-friendly Version](#)

[Interactive Discussion](#)



know from Fig. 2b that the AKR is actually observed around 192 kHz. Simply adding the conversion factor of 125 kHz to the frequency of the AKR obtained with the baseband time scale (66.7 kHz) yields the expected frequency of the AKR of 192 kHz.

The pulse observed in Fig. 2a has a time duration of 27 μ s (start of pulse rise from base field to end of pulse fall at base field). If we think of this as a one-period wave, the inverse time duration would give us a frequency of 37.037 kHz. Adding 125 kHz to this frequency yields a frequency of \sim 162 kHz and thus fits within the sampled conversion frequency range of 125–202 kHz, and so we are not surprised that the pulse survived the down conversion process.

This now brings us to the problem at hand. What is the true characteristic time scale of the pulse? Can we actually view it as a one-period wave and thus determine its characteristic time duration as it was sampled onboard before down conversion? Before down conversion, did the pulse actually have the form of a bipolar pulse (negative peak followed by a positive peak of similar amplitude, or vice versa), or did it possibly have some other embedded frequencies or structure which after mixing and down conversion produced the signature of a classical bipolar pulse (see e.g., Pickett et al., 2004a)? To help answer these questions, we now look to the simulations.

3 Simulations of conversion mode

In order to simulate the mixing and down conversion process that takes place within the WBD instrument, we first synthesized a very high time resolution digital waveform example and then performed the down conversion on this signal.

3.1 Constructed signal

In seeking a form for our constructed signal, recall the previous section's discussion of the pulse found in the sample of actual WBD data. It was observed that if the pulse was thought of as a one-period wave, then the calculated "frequency" of the pulse (37 kHz)

Interpretation of Cluster WBD frequency conversion mode data

J. S. Pickett et al.

[Title Page](#)

[Abstract](#)

[Introduction](#)

[Conclusions](#)

[References](#)

[Tables](#)

[Figures](#)



[Back](#)

[Close](#)

[Full Screen / Esc](#)

[Printer-friendly Version](#)

[Interactive Discussion](#)



Interpretation of Cluster WBD frequency conversion mode data

J. S. Pickett et al.

[Title Page](#)

[Abstract](#)

[Introduction](#)

[Conclusions](#)

[References](#)

[Tables](#)

[Figures](#)

[⏪](#)

[⏩](#)

[◀](#)

[▶](#)

[Back](#)

[Close](#)

[Full Screen / Esc](#)

[Printer-friendly Version](#)

[Interactive Discussion](#)



was consistent with a 125 kHz down conversion (the original “frequency” of the pulse was calculated as 162 kHz, which is within the 125 to 202 kHz range of the conversion band/bandwidth being used). Taking this thought one step further, we can think of the observed pulse as a narrow wave packet, so narrow that the envelope of the packet contains only a single period of an approximately pure sinusoid, which we call the carrier wave. For discussion, let us say that the packet is 30 μs in length. Since the goal of the down conversion process is, in essence, to preserve the envelope of waveforms (i.e., the information content of the waveform), while shifting the carrier frequency lower, we can presume that the original (pre-conversion) waveform also contained a 30 μs wave packet, but with a carrier wave frequency around 162 kHz, as calculated above. We take this to be the starting point for our simulations.

We construct a Gaussian wave packet of the following form:

$$P(t) = A \sin(2\pi Ft + \varphi) e^{-(t/\tau)^2} \quad (1)$$

where A is the packet amplitude, F and φ are the frequency and phase of the carrier wave, respectively, and $\tau = W/3 \times 10^6$ (W is the width parameter, which sets the approximate width of the packet, in μs). A packet using $A = 10$, $W = 30 \mu\text{s}$, $F = 162 \text{ kHz}$ and $\varphi = 0$ is shown in Fig. 3a, and the Fourier transform of this packet is shown in Fig. 4a. Note that much of the spectral energy of this waveform is contained within our conversion band (125 to 202 kHz), which gives us confidence that much of the information contained in the packet will survive the down conversion process.

3.2 Down converted signal

The down conversion process, performed via analog quadrature mixing circuitry in the instrument, is now applied to our constructed signal. The down conversion from a base of 125 kHz to baseband of 0 kHz is simulated by doing the quadrature mixing with a Hilbert Transform (HT). This mixing could also have been simulated by an FIR (Finite Impulse Response) filter, but we have chosen to use an HT since it is inherently simpler,

while creating an FIR filter to deal with our complex signals can be quite difficult to achieve.

Figure 3b shows the waveform from Fig. 3a, after it has been down converted using the above process. The result is a signature very like a bipolar pulse, with an amplitude that is close to 80% of the input amplitude, and a width that is almost exactly the same as that of the input packet. Measuring the period of the sinusoid, we see that it is slightly under the 30 μ s, width of the original packet, giving a frequency of \sim 35 kHz. Adding 125 kHz to this recovers the original carrier frequency of 162 kHz, within our measurement uncertainty. We thus confirm that a wave packet, at least in some circumstances, will be down converted into a waveform that resembles a bipolar pulse.

3.3 Other constructed waveforms

The next question to ask is if this is the only initial waveform that could result in such a bipolar output after down conversion. Figure 4a showed the spectral energy that is *necessary* to produce the down converted waveform seen in Fig. 3b, but if we recall that the down conversion process is designed to discard all spectral energy outside of the band (as well as down shifting the energy within the band), then any spectral signature that fills much or all of the 125 to 202 kHz band may do the same.

Consider now an input waveform that is an actual, very narrow, bipolar pulse, such as the 6 μ s pulse shown in Fig. 3c. This pulse is defined by:

$$P(F) = E \left(\frac{T}{\tau/100} \right) / \cosh \left(\frac{T}{\tau/100} \right) e^{-(T/\tau)^2} \quad (2)$$

where $E = 2AP$ (A is the amplitude and $P = \pm 1$ sets the polarity of the pulse), and $\tau = W/80,000$. The spectral profile of this pulse is the black line shown in Fig. 4b, which is very broad, as expected, given the very short, sharp nature of the pulse. If we were to apply a 125 to 202 kHz bandpass filter to this waveform (thus estimating the spectral energy that would survive down conversion), the energy that remains is shown by the

Interpretation of Cluster WBD frequency conversion mode data

J. S. Pickett et al.

[Title Page](#)

[Abstract](#)

[Introduction](#)

[Conclusions](#)

[References](#)

[Tables](#)

[Figures](#)

[⏪](#)

[⏩](#)

[◀](#)

[▶](#)

[Back](#)

[Close](#)

[Full Screen / Esc](#)

[Printer-friendly Version](#)

[Interactive Discussion](#)



Interpretation of Cluster WBD frequency conversion mode data

J. S. Pickett et al.

[Title Page](#)

[Abstract](#)

[Introduction](#)

[Conclusions](#)

[References](#)

[Tables](#)

[Figures](#)

[⏪](#)

[⏩](#)

[◀](#)

[▶](#)

[Back](#)

[Close](#)

[Full Screen / Esc](#)

[Printer-friendly Version](#)

[Interactive Discussion](#)

time of the injected pulse. A pulse of $5\ \mu\text{s}$ in duration is seen in the middle of the sample, at $t = 100\ \mu\text{s}$, with an amplitude of 10 a.u. (arbitrary units), while the background noise and other sinusoidal signals are seen throughout, centered at 0 amplitude with a net amplitude of 1–1.5 a.u. An FFT of the full constructed waveform is shown in Fig. 5b.

This frequency-time spectrogram covers a period of about 5 ms, which is comparable to a single frame obtained by the WBD instrument using the 77 kHz filter bandwidth with a 125 kHz conversion. Here we clearly see two sinusoidal waves showing up with medium amplitudes around 140 and 150 kHz, similar to AKR frequencies, as well as some weaker waves at and above 175 kHz, throughout the plot. The single injected pulse is observed as a broad band around 0.0023 s.

Figure 5c is the same 5 ms constructed waveform as that seen in Fig. 5a with the exception that it has been mixed and down converted using the HT. We can immediately see the effects of this process in the waveform. The sinusoidal waves and background noise have been smoothed out, and the pulse has been greatly reduced in amplitude (now about 2.5 a.u.) and stretched out in time (time duration now about $15\ \mu\text{s}$). However, the stretch out in time is consistent with the filter bandwidth (77 kHz) and is expected for the pulse as discussed earlier in this section. Because of the decreased amplitude it is not possible to determine the period of the sinusoidal waves, because we have down converted to the time scale of baseband (0 kHz base frequency).

Figure 5d thus shows an FFT spectrogram of the waveform seen in Fig. 5c now with a frequency range from 0 to 77 kHz. When we compare this spectrogram to the one prior to down conversion (Fig. b), we see that all of the frequency information has been precisely preserved, including the pulse, and that no frequency content from outside our desired band has been shifted into the band. However, some low frequency noise at the bottom of the frequency band has been artificially introduced during the down conversion process.

4 Interpretation and guidance

Several waveform data samples containing noise, sinusoidal waves and pulses were constructed as discussed in Sect. 3. Using a Hilbert Transform to mix and down convert the constructed waveforms to a base frequency of 0 kHz, we have demonstrated that (1) sinusoidal waves will be represented as sine waves with periods consistent with the original frequency shifted down by the conversion factor (in our case 125 kHz), and (2) pulses and wave packet bursts with sufficient amplitudes will be down converted to the base frequency with time scales that to a large degree result from the filter bandwidth that was selected (for example, inverting 77 kHz gives a time scale of $\sim 13 \mu\text{s}$). We can thus generalize the results obtained in Sect. 3 and apply them to the Cluster WBD data by saying that if the incident waveform contains any short (less than 20–30 μs in duration), intense (relative to any other ambient signal) pulse, of any particular shape, then it will have a broad spectral profile. Such a profile will likely fill the Cluster WBD 125 to 202 kHz frequency band with energy, and thus will result in a bipolar-like structure (specifically roughly one period of a sinusoidal wave packet) in the down converted waveform. These bipolar-like structures are likely to have apparent widths ranging from $\sim 30 \mu\text{s}$ down to the digitization limit of the instrument (15–20 μs). Note that if the input pulse is *too* short, less than a microsecond or so, then much of the spectral energy has shifted above 202 kHz, so again there will not be much energy that survives the down conversion process. At the other end of the time scale, it should be noted that the multipole filters used within the WBD instrument to select each of the three filter bandwidths can distort pulses which are too long in duration (see Swanner et al., 2006). As discussed above, though, such pulses would only be observed in data taken in baseband mode.

In contrast to pulse-like structures, sinusoidal waves with frequencies that fall within the selected conversion band will be down converted to base frequency with nearly 100 % of their original energy retained, as per the design of the WBD instrument. The apparent frequency of these waves, when seen as waveforms, will be that of their orig-

GID

3, 547–565, 2013

Interpretation of Cluster WBD frequency conversion mode data

J. S. Pickett et al.

[Title Page](#)

[Abstract](#)

[Introduction](#)

[Conclusions](#)

[References](#)

[Tables](#)

[Figures](#)

[⏪](#)

[⏩](#)

[◀](#)

[▶](#)

[Back](#)

[Close](#)

[Full Screen / Esc](#)

[Printer-friendly Version](#)

[Interactive Discussion](#)



inal frequency, minus the conversion ($\sim 125, 250$ or 500 kHz). Their true (i.e., original) frequencies are easily recovered after transforming the waveforms into the frequency domain (via FFT), by upshifting each displayed frequency by that same amount.

Historically, broad band signals have often been seen in the spectrograms of AKR as observed from space (such as that seen in Fig. 2). Most of those data were obtained in the spectral domain. Thus, there was no way to determine the source of those broad bands. With the advent of waveform receivers with high sampling rates, we have learned that those broad bands, at least when observed at the base frequency, often are indicative of electrostatic structures such as electron phase space holes which are created out of nonlinear processes (e.g., Pickett et al., 2004a, b). Knowing now that similar broad band signals in conversion mode data could possibly indicate the presence of similar type structures, or impulsive, nonlinear type wave packets, we can now more effectively analyse AKR data obtained in the auroral acceleration region, or in any other magnetospheric region. By noting their presence, we can use this knowledge when analyzing the generation of AKR, particularly its fine structure, and other auroral processes.

As a final note, it may be that more in depth illumination of the complications involved in interpreting pulse-like structures in conversion mode data could be obtained from the field of astronomy. Astronomers have typically used similar and more complex methods in analysing data from pulsars where the time periods of the signal pulse received from the pulsar is so short that sampling of the signal must take place at very high rates with subsequent down conversion (see e.g., Hankins et al., 1975). It is possible that a study of these techniques could lead to methods that would allow more to be learned about the pulses and/or impulsive wave packets that are the source of the structures and broad band signals seen in the WBD conversion mode data. However, we stress that the original waveforms, whether input pulses and wave packets or pure sinusoids, are never preserved or recorded by WBD when using down conversion. Thus the exact structure of the original input waveform can never be known or recovered from the

Interpretation of Cluster WBD frequency conversion mode data

J. S. Pickett et al.

[Title Page](#)

[Abstract](#)

[Introduction](#)

[Conclusions](#)

[References](#)

[Tables](#)

[Figures](#)

[⏪](#)

[⏩](#)

[◀](#)

[▶](#)

[Back](#)

[Close](#)

[Full Screen / Esc](#)

[Printer-friendly Version](#)

[Interactive Discussion](#)



down converted waveform from Cluster WBD or from any similar waveform instrument using down conversion techniques.

Acknowledgements. We acknowledge support from NASA Goddard Space Flight Center under grant NNX11AB38G. We also acknowledge fruitful discussions with R. L. Huff and J. R. Phillips from The University of Iowa in helping us to understand the frequency conversion mode through bench tests with the flight spare WBD receiver.

References

- Gurnett, D. A., Huff, R. L., and Kirchner, D. L.: The Wide-Band Plasma Wave Investigation, *Space Sci. Rev.*, 79, 195–208, 1997.
- Hankins, T. H. and Rickett, B. J.: Pulsar signal processing, *Meth. Comp. Phys.* 14, 55–129, 1975.
- Norgaard, E. E.: The phase-shift method of single-sideband signal generation, *Proc. IRE*, 44, 1735–1743, 1956.
- Pickett, J. S., Chen, L.-J., Kahler, S. W., Santolík, O., Gurnett, D. A., Tsurutani, B. T., and Balogh, A.: Isolated electrostatic structures observed throughout the Cluster orbit: relationship to magnetic field strength, *Ann. Geophys.*, 22, 2515–2523, doi:10.5194/angeo-22-2515-2004, 2004a.
- Pickett, J. S., Kahler, S. W., Chen, L.-J., Huff, R. L., Santolík, O., Khotyaintsev, Y., Décréau, P. M. E., Winningham, D. Frahm, R., Goldstein, M. L., Lakhina, G. S., Tsurutani, B. T., Lavraud, B., Gurnett, D. A., André, M., Fazakerley, A., Balogh, A., and Rème, H.: Solitary waves observed in the auroral zone: the Cluster multi-spacecraft perspective, *Nonlinear Proc. Geophys.*, 11, 183–196, 2004b.
- Swanner, J. M., Pickett, J. S., Phillips, D. L., and Kirchner, D. L.: WBD response to bipolar and tripolar pulses: bench tests vs. in flight observations, available at: www-pw.physics.uiowa.edu/cluster/pulse_tests.pdf and caa.estec.esa.int (last access for both links: 21 August 2013) (in Documentation section for WBD), 2006.

Interpretation of Cluster WBD frequency conversion mode data

J. S. Pickett et al.

[Title Page](#)

[Abstract](#)

[Introduction](#)

[Conclusions](#)

[References](#)

[Tables](#)

[Figures](#)

[⏪](#)

[⏩](#)

[◀](#)

[▶](#)

[Back](#)

[Close](#)

[Full Screen / Esc](#)

[Printer-friendly Version](#)

[Interactive Discussion](#)



Interpretation of Cluster WBD frequency conversion mode data

J. S. Pickett et al.

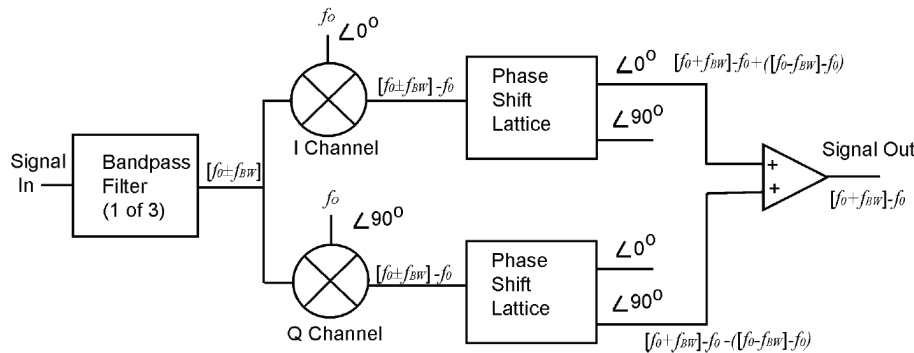


Fig. 1. Diagram showing the Cluster WBD frequency conversion chain for down converting a signal received at higher frequency $[f_0 + f_{BW}]$ to one at baseband frequency ($f_0 = 0$).

Title Page

Abstract	Introduction
Conclusions	References
Tables	Figures

⏪
⏩

◀
▶

Back	Close
------	-------

Full Screen / Esc

Printer-friendly Version

Interactive Discussion

Interpretation of Cluster WBD frequency conversion mode data

J. S. Pickett et al.

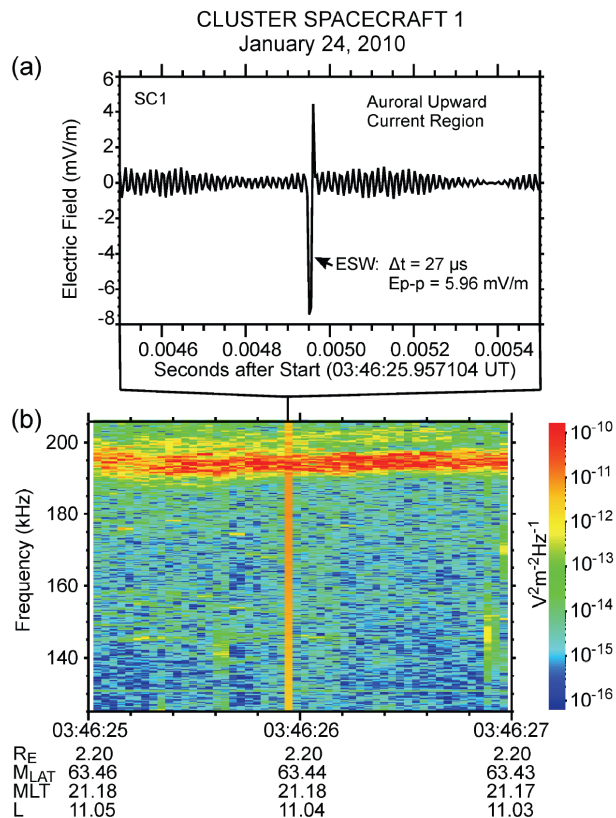


Fig. 2. WBD data obtained from Cluster 1 on 24 January 2010 in the auroral upward current region. **(a)** 1 ms duration waveform showing sinusoidal waves and a bipolar pulse. **(b)** 2 s frequency-time spectrogram showing that the sinusoidal waves represent AKR around 192 kHz and the pulse represents the broad band observed just before 03:46:26 UT.

[Title Page](#)

[Abstract](#)

[Introduction](#)

[Conclusions](#)

[References](#)

[Tables](#)

[Figures](#)

[⏪](#)

[⏩](#)

[◀](#)

[▶](#)

[Back](#)

[Close](#)

[Full Screen / Esc](#)

[Printer-friendly Version](#)

[Interactive Discussion](#)

Interpretation of Cluster WBD frequency conversion mode data

J. S. Pickett et al.

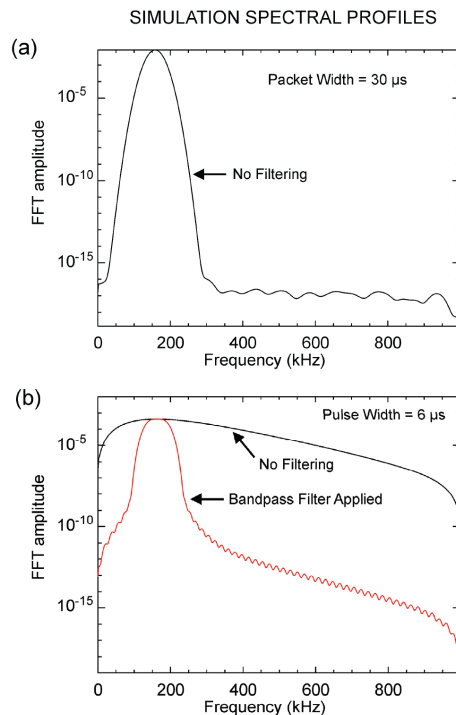


Fig. 4. Spectral profiles (amplitude vs. frequency) of simulated waveform data from Fig. 2 before down conversion. **(a)** Spectrum of the waveform packet presented in Fig. 3a showing a spectral peak at about 160 kHz, the energy being almost fully contained within the 125–202 kHz frequency band. **(b)** Black line: spectrum of the pulse presented in Fig. 3c showing a broad band nearly covering the entire Fourier frequency space, with much of the energy outside the 125–202 kHz frequency band; Red line: spectrum of the pulse after filtering down to the 125–202 kHz frequency band, to show comparison with the profile in Fig. 4a.

[Title Page](#)[Abstract](#)[Introduction](#)[Conclusions](#)[References](#)[Tables](#)[Figures](#)[◀](#)[▶](#)[◀](#)[▶](#)[Back](#)[Close](#)[Full Screen / Esc](#)[Printer-friendly Version](#)[Interactive Discussion](#)

Interpretation of Cluster WBD frequency conversion mode data

J. S. Pickett et al.

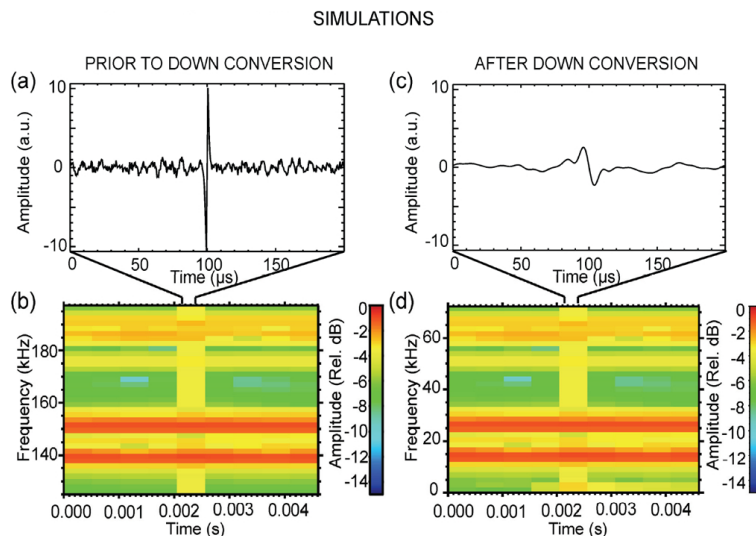


Fig. 5. Simulated data both before and after down conversion for comparison to space observations shown in Fig. 2. **(a)** 200 μs sample of the input waveform showing the 5 μs constructed pulse, as well as sinusoidal oscillations and background noise, prior to down conversion. **(b)** 5 ms time-frequency spectrogram of the simulated data shown in **(a)**. **(c)** 200 μs sample of the waveform presented in **(a)**, after having been down converted from the frequency range 125–202 kHz to baseband; the sinusoidal waves have been smoothed out and time dilated by the process; the pulse has been reduced in amplitude, and broadened in time, consistent with the effects of the 77 kHz band filter. **(d)** 5 ms time-frequency spectrogram of the down converted waveform in **(c)** showing the broad band associated with the pulse, and the sinusoidal waves on the down converted frequency scale.

[Title Page](#)
[Abstract](#)
[Introduction](#)
[Conclusions](#)
[References](#)
[Tables](#)
[Figures](#)
[◀](#)
[▶](#)
[◀](#)
[▶](#)
[Back](#)
[Close](#)
[Full Screen / Esc](#)
[Printer-friendly Version](#)
[Interactive Discussion](#)